



Highly functionalized pyranopyrazoles: synthesis, antimicrobial activity, simulation studies and their structure activity relationships (SARs)

Guda Mallikarjuna Reddy^{1,2} · Gundala Sravya² · Gutha Yuvaraja³ · Alexandre Camilo Jr.⁴ · Grigory V. Zyryanov^{2,5} · Jarem Raul Garcia¹

Received: 6 June 2018 / Accepted: 16 August 2018
© Springer Nature B.V. 2018

Abstract

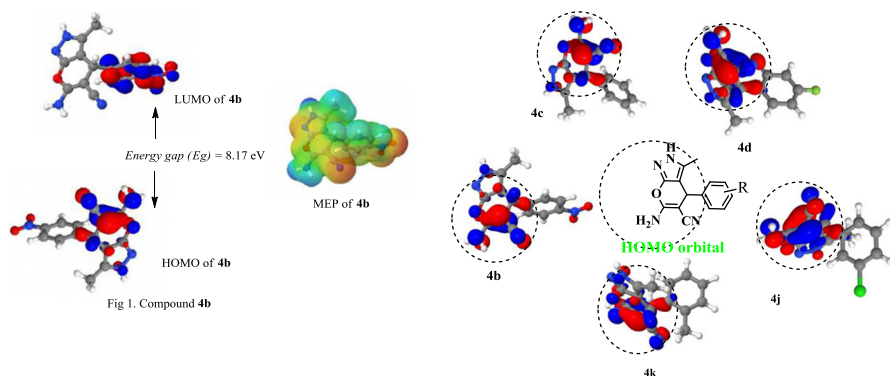
Development of potent antibacterial and antifungal agents is a permanently new and unremitting investigation in the therapeutic field. Still, medicinal research wants to find the best antimicrobial agent. To attain this goal, here, the present work synthesis, simulation, and antimicrobial studies of pyranopyrazole derivatives were discussed. Among the reported compounds, **4b** has dominant antimicrobial activity that was due to its higher dipole moment. Also, this compound has the most hydrophilic nature and low E_g value. Besides, compound **4e** has the next higher dipole moment, hydrophilic property and efficient biological activity. The rationale of these results explained that the comparison of electronic results with biological data is the better way to find the potent pharmaceutical drug compounds.

Electronic supplementary material The online version of this article (<https://doi.org/10.1007/s11164-018-3569-8>) contains supplementary material, which is available to authorized users.

✉ Jarem Raul Garcia
nagareddy.organic@gmail.com

Extended author information available on the last page of the article

Graphical abstract



Keywords Microwave synthesis · Antimicrobial activity · SARs · HOMO–LUMO · Energy gap · Electronic parameters

Introduction

In and around 1980 there was a slogan, “now the time to close the volume on bacterial sickness as the main health risk” by US doctors. At that time antibiotic drugs were considered to create a sensation. Later, the resistance to antibiotics is the major problem facing us now everywhere. Novel therapy agents are needed to fight these microbial pathogens, for this, the detection of new platforms should be an important phenomenon [1, 2]. Countless heterocycles were shown to be in biological and pharmacological actions. In that, 2-pyrones and their fused derivatives have fascinated us due to their biotic activities [3–5]. In addition, pyrazoles act as a core nucleus in various drugs due to their actions such as antimicrobials [6], antioxidants [7, 8] cytotoxicity [9], and other properties [10]. The combination of two heterocycles into one molecule could afford a novel entity with increase bioactivities [11–18]. On the way, dihydro-1*H*-pyrano[2,3-*c*]pyrazoles signify a motivating template in therapeutic chemistry and play an essential role in the pharmaceutical field. Such compounds displayed biological activities like antifungal, antibacterial, anticancer and antiinflammatory [19, 20]. Recently, Yang et al, stated some pyranopyrazoles have good antioxidant and cytotoxicity properties [21]. Additionally, the most vital aspect is SARs, and it has become helpful in understanding numerous aspects of chemical–biological interactions in drug, pesticide research and other areas. In a way, an electronic structure of a compound displays a fundamental role in a mechanism associated with biological and pharmacological activities [22]. Yan et al., explained the theoretical calculations, biological assay and their relationships of pyrazole derivatives [23]. Thus, electronic properties such as the molecular electrostatic profile (MESP), the lowest

unoccupied molecular orbital (LUMO), the highest occupied molecular orbital (HOMO), energy gap, and dipole moment are useful parameters for an accurate understanding of the chemical reactivity of molecules [24–30]. Peculiarly, MESP has proven a tool for exploring molecular electronic structure, reactivity patterns, and structure–activity relationship studies [31–33].

Herein, we report a microwave synthetic method, theoretical calculations and antimicrobial activity of the pyranopyrazole derivatives. To identify the potent antimicrobial agent, structure–activity relationships allowed a correct correlation of biological activity with some appropriate quantum descriptors such as HOMO, LUMO, energy gap and dipole moment.

Experimental data

General

Computational methodology and chemistry

By using the Density Functional Theory (DFT) method, electronic parameters such as Molecular Electrostatic Potential (MEP), dipole moment, HOMO (Highest Occupied Molecular Orbital), LUMO (Lowest Unoccupied Molecular Orbitals) and heat of formation (HF) were calculated for all the reported compounds. These calculations were calculated from all electronic energies of the cationic (E^+), anionic (E^-) and neutral (E^0) representations. For DFT calculations executed on the GAMESS-US [34] line up package, for Iodine atom, SPK-DZP (Sapporo Double Zeta Potential) [35] basis set was applied, and 6-31+G(p) basis set, and B3LYP hybrid functional were applied for atoms like Cl, C, S, O, H, N, and F. In relation of entire system energy, the compound structure was completely relaxed. Proton NMR and carbon NMR data were noted at 500 MHz and 75 MHz. Internal standards were tetramethylsilane. Melting point statistics were pointed out with a micromelting point device and were uncorrected. Synthetic methods were performed in a microwave oven, Catalyst-4R. The mass spectra were recorded on Jeol JMS-D 300 and Finnigan Mat 1210 B mass spectrometers at 70 eV with an emission current of 100 μ A. The elemental analysis was determined by using Perkin-Elmer 240C elemental analyzer. HRMS data and was obtained using Electro spray ionization (ESI).

Protocol for the preparation of pyranopyrazole derivatives (4a–m)

Substituted aromatic aldehyde (**1a**) (1.0 mmol) and malononitrile (**2**) (1.0 mmol) were added to the ethanol solution (5 mL) consisting of methyl-1*H*-pyrazol-5(4*H*)-one (1.0 mmol) (**3**). The total reaction blend was irradiated with microwaves for 10 min at 130 °C (250 W). The reaction monitored, and product confirmation was observed by TLC. Then, the crud was poured into chilled ice, extracted with dichloromethane, and concentrated by rotary evaporation. The residue was purified by silica gel column chromatography with hexane–EtOAc (4:1) as eluent to afford

final compound **4a**. All the other products were followed by the same procedure with their respective starting material.

4-(p-Tolyl)-3-methyl-6-amino-2,4-dihydropyrano[2,3-c]pyrazole-5-carbonitrile (4a)

Off white solid in (0.26 g, 85%); M.p. 212–214 °C; ^1H NMR (500 MHz, $\text{CDCl}_3 + \text{DMSO}-d_6$): δ 2.04 (s, 3H, CH_3), 2.49 (s, 3H, Ar- CH_3), 4.71 (s, 1H, 4H), 5.53 (s, 2H, NH_2), 7.22–7.61 (m, 4H, Ar-H), 11.59 (s, 1H, NH) ppm; ^{13}C NMR (75 MHz, $\text{DMSO}-d_6$): δ 9.6, 20.5, 35.7, 57.3, 97.6, 117.1, 120.6, 127.2, 128.8, 135.4, 141.3, 154.6, 160.6 ppm; MS m/z : 266.11 (M +). Anal. Calcd for $\text{C}_{15}\text{H}_{14}\text{N}_4\text{O}$: C, 67.65; H, 5.30; N, 21.04; Found: C, 67.59; H, 5.24; N, 21.01; HRMS (ES^+) Calcd for (M + H) $^+$ 267.12404 found m/z 267.1235.

4-(4-Nitrophenyl)-6-amino-3-methyl-2,4-dihydropyrano[2,3-c]pyrazole-5-carbonitrile (4b)

White solid in (0.29 g, 91%); M.p. 263–265 °C; ^1H NMR (500 MHz, $\text{DMSO}-d_6$): δ 1.40 (s, 3H, CH_3), 4.31 (s, 1H, 4H), 5.50 (s, 2H, NH_2), 7.02 (d, 2H, Ar-H, $J = 12.5 \text{ Hz}$), 7.71 (d, 2H, Ar-H, $J = 12.5 \text{ Hz}$), 11.43 (s, 1H, NH) ppm; ^{13}C NMR (75 MHz, $\text{DMSO}-d_6$): δ 9.6, 35.7, 55.8, 96.4, 120.3, 123.7, 128.7, 135.7, 146.2, 151.9, 154.5, 161.0 ppm; MS m/z : 297.08 (M +). Anal. Calcd for $\text{C}_{14}\text{H}_{11}\text{N}_5\text{O}_3$: C, 56.56; H, 3.73; N, 23.56; Found: C, 56.62; H, 3.85; N, 23.61; HRMS (ES^+) Calcd for (M + H) $^+$ 298.09347 found m/z 298.0929.

4-Phenyl-6-amino-3-methyl-2,4-dihydropyrano[2,3-c]pyrazole-5-carbonitrile (4c)

White solid in (0.25 g, 88%); M.p. 174–177 °C; ^1H NMR (500 MHz, $\text{DMSO}-d_6$): δ 1.78 (s, 3H, CH_3), 3.99 (s, 1H, NH), 4.96 (s, 1H, 4H), 6.98–7.06 (m, 2H, Ar-H), 7.15–7.25 (m, 3H, Ar-H) ppm; ^{13}C NMR (75 MHz, $\text{DMSO} + \text{CDCl}_3-d_6$): δ 9.5, 26.8, 42.4, 48.6, 97.9, 112.7, 127.2, 127.4, 128.3, 138.5, 159.4, 174.0 ppm; MS m/z : 252.10 (M +). Anal. Calcd for $\text{C}_{14}\text{H}_{12}\text{N}_4\text{O}$: C, 66.65; H, 4.79; N, 22.21; Found: C, 66.48; H, 4.62; N, 22.14; HRMS (ES^+) Calcd for (M + H) $^+$ 253.10839 found m/z 253.1079.

(4-Fluorophenyl)-6-amino-4-methyl-2,4-dihydropyrano[2,3-c]pyrazole-5-carbonitrile (4d)

Light yellow solid in (0.27 g, 90%); M.p. 242–244 °C; ^1H NMR (500 MHz, $\text{DMSO}-d_6$): δ 1.42 (s, 3H, CH_3), 4.21 (s, 1H, 4H), 5.30 (s, 2H, NH_2), 6.50–6.79 (m, 4H, Ar-H) ppm; ^{13}C NMR (75 MHz, $\text{DMSO} + \text{CDCl}_3-d_6$): δ 9.4, 35.5, 59.0, 96.7, 114.4, 114.6, 119.9, 128.5, 135.5, 138.8, 160.0 ppm; MS m/z : 270.09 (M +). Anal. Calcd for $\text{C}_{14}\text{H}_{11}\text{FN}_4\text{O}$: C, 62.22; H, 4.10; N, 20.73; Found: C, 62.18; H, 3.98; N, 20.71; HRMS (ES^+) Calcd for (M + H) $^+$ 271.09897 found m/z 271.0984.

3-Methyl-6-amino-4-((4-trifluoromethyl)phenyl)-2,4-dihydropyrano[2,3-c]pyrazole-5-carbonitrile (4e)

Yellow solid in (0.32 g, 84%); M.p. 191–193 °C; ^1H NMR (500 MHz, $\text{DMSO}-d_6$): δ 2.11 (s, 3H, CH_3), 4.16 (s, 1H, 4H), 5.17 (b, 1H, NH), 6.70–6.75 (d, 2H, Ar-H, $J = 12.3 \text{ Hz}$), 7.34–7.36 (d, 2H, Ar-H, $J = 13.0 \text{ Hz}$) ppm; ^{13}C NMR (75 MHz, $\text{DMSO} + \text{CDCl}_3-d_6$): δ 9.6, 27.4, 42.1, 55.5, 98.0, 113.8, 114.5, 122.1, 128.9, 131.8, 133.1, 138.5, 159.3, 165.1 ppm; MS m/z : 320.08 (M +). Anal. Calcd for $\text{C}_{15}\text{H}_{11}\text{F}_3\text{N}_4\text{O}$: C, 56.25; H, 3.46; N, 17.49; Found: C, 56.31; H, 3.56; N, 17.60; HRMS (ES^+) Calcd for (M + H) $^+$ 321.2692 found m/z 321.2698.

3-Methyl-6-amino-4-(4-chlorophenyl)-2,4-dihydropyrano[2,3-c]pyrazole-5-carbonitrile (4f) Light yellow solid in (0.28 g, 89%); M.p. 160–162 °C; ^1H NMR (500 MHz, DMSO- d_6): δ 1.90 (s, 3H, CH₃), 3.88 (s, 1H, 4H), 4.65 (s, 1H, NH), 6.62–6.72 (m, 4H, Ar–H) ppm; ^{13}C NMR (75 MHz, DMSO- d_6): δ 9.5, 16.9, 48.7, 97.4, 112.5, 128.3, 128.9, 133.0, 137.1, 138.7, 159.4 ppm; MS m/z : 286.06 (M +). Anal. Calcd for C₁₄H₁₁ClN₄O: C, 58.65; H, 3.87; N, 19.54; Found: C, 58.51; H, 3.76; N, 19.36; HRMS (ES⁺) Calcd for (M + H)⁺ 287.06942 found m/z 287.0688.

3-Methyl-6-amino-4-(4-bromophenyl)-2,4-dihydropyrano[2,3-c]pyrazole-5-carbonitrile (4g) Yellow solid in (0.33 g, 92%); M.p. 172–174 °C; ^1H NMR (500 MHz, DMSO- d_6): δ 1.83 (3H, CH₃, S), 3.91 (d, 1H, 4H), 4.72 (d, 1H, NH), 6.61–6.69 (m, 4H, Ar–H) ppm; ^{13}C NMR (75 MHz, DMSO- d_6): δ 9.5, 16.4, 47.9, 97.0, 113.4, 129.3, 129.5, 132.5, 135.4, 138.5, 155.4 ppm; MS m/z : 330.01 (M +). Anal. Calcd for C₁₄H₁₁BrN₄O: C, 50.77; H, 3.35; N, 16.92; Found: C, 50.81; H, 3.49; N, 17.03; HRMS (ES⁺) Calcd for (M + H)⁺ 332.1673 found m/z 332.1370.

3-Methyl-6-amino-4-(2-bromophenyl)-2,4-dihydropyrano[2,3-c]pyrazole-5-carbonitrile (4h) Light yellow solid in (0.33 g, 81%); M.p. 232–235 °C; ^1H NMR (500 MHz, DMSO- d_6): δ 1.85 (s, 3H, CH₃), 3.87 (d, 1H, 4H), 4.69 (d, 1H, NH), 6.61–6.74 (m, 4H, Ar–H), ppm; ^{13}C NMR (75 MHz, DMSO- d_6): δ 9.4, 16.5, 47.1, 95.9, 115.1, 126.0, 129.8, 134.5, 138.4, 139.4, 158.5 ppm; MS m/z : 330.01 (M +). Anal. Calcd for C₁₄H₁₁BrN₄O: C, 50.77; H, 3.35; Br, 24.13; N, 16.92; Found: C, 50.68; H, 3.32; N, 16.88; HRMS (ES⁺) Calcd for (M + H)⁺ 332.1673 found m/z 332.1652.

3-Methyl-6-amino-4-(2-fluorophenyl)-2,4-dihydropyrano[2,3-c]pyrazole-5-carbonitrile (4i) Light yellow solid in (0.27 g, 83%); M.p. 214–216 °C; ^1H NMR (500 MHz, DMSO- d_6): δ 1.63 (s, 3H, CH₃), 4.20 (s, 1H, 4H), 5.28 (s, 2H, NH₂), 6.59 (q, 2H, Ar–H, $J = 12.3$ Hz), 6.90 (t, 2H, Ar–H, $J = 12.3$ Hz) ppm; ^{13}C NMR (75 MHz, DMSO + CDCl₃- d_6): δ 9.6, 27.0, 34.5, 61.0, 94.1, 115.4, 117.2, 121.6, 127.9, 135.0, 139.2, 158.9 ppm; MS m/z : 270.09 (M +). Anal. Calcd for C₁₄H₁₁FN₄O: C, 62.22; H, 4.10; N, 20.73; Found: C, 62.19; H, 4.15; N, 20.65; HRMS (ES⁺) Calcd for (M + H)⁺ 271.09897 found m/z 271.0984.

3-Methyl-6-amino-4-(3-Chlorophenyl)-2,4-dihydropyrano[2,3-c]pyrazole-5-carbonitrile (4j) Light yellow solid in (0.28 g, 92%); M.p. 181–183 °C; ^1H NMR (300 MHz, DMSO- d_6): δ 1.29 (s, 3H, CH₃), 4.11 (s, 1H, 4H), 5.46 (s, 2H, NH₂), 6.76–6.99 (m, 2H, Ar–H), 7.69 (t, 2H, Ar–H, $J = 13.5$ Hz), ppm; ^{13}C NMR (75 MHz, DMSO + CDCl₃- d_6): δ 9.5, 35.4, 58.6, 96.2, 120.4, 122.3, 125.8, 129.1, 132.5, 137.5, 143.2, 145.7, 156.5, 162.3 ppm; MS m/z : 286.06 (M +). Anal. Calcd for C₁₄H₁₁ClN₄O: C, 58.65; H, 3.87; N, 19.54; Found: C, 58.69; H, 4.01; N, 19.58; HRMS (ES⁺) Calcd for (M + H)⁺ 287.7163 found m/z 286.7058.

3-Methyl-6-amino-4-(2-aminophenyl)-2,4-dihydropyrano[2,3-c]pyrazole-5-carbonitrile (4k) Yellow solid in (0.26 g, 89%); M.p. 201–203 °C; ^1H NMR (500 MHz, CDCl₃ + DMSO- d_6): δ 1.80 (s, 3H, CH₃), 5.20 (t, 3H, 4H + NH₂, $J = 12.5$ Hz), 6.06 (bs, 2H, NH₂), 7.19–7.35 (m, 1H, Ar–H), 7.47–7.88 (m, 3H, Ar–H) ppm; ^{13}C NMR (75 MHz, DMSO- d_6): δ 9.5, 27.4, 48.9, 97.2, 114.5, 125.1, 128.1, 129.2,

132.0, 133.2, 138.9, 149.3, 159.4, 172.6 ppm; MS m/z : 267.11 (M^+). Anal. Calcd for $C_{14}H_{13}N_5O$: C, 62.91; H, 4.90; N, 26.20; Found: C, 62.84; H, 4.79; N, 26.16; HRMS (ES^+) Calcd for $(M + H)^+$ 268.2859 found m/z 268.2796.

3-Methyl-6-amino-4-(2-iodophenyl)-2,4-dihydropyrano[2,3-c]pyrazole-5-carbonitrile (4I)

Light yellow solid in (0.37 g, 90%); M.p. 212–214 °C; 1H NMR (500 MHz, CD_3OD-d_4): δ 1.83 (s, 3H, CH_3), 4.56 (s, 1H, 4H), 6.41–6.70 (m, 3H, Ar-H), 7.17 (t, 1H, Ar-H, $J = 12.5$ Hz) ppm; ^{13}C NMR (75 MHz, CD_3OD-d_4): δ 9.7, 35.2, 82.8, 115.8, 116.5, 117.5, 122.4, 127.9, 131.5, 1357.3, 145.2, 153.4, 157.2, 160.5 ppm; MS m/z : 377.99 (M^+). Anal. Calcd for $C_{14}H_{11}IN_4O$: C, 44.46; H, 2.93; N, 14.82; Found: C, 44.39; H, 2.85; N, 14.75; HRMS (ES^+) Calcd for $(M + H)^+$ 378.1678 found m/z 378.1596.

3-Methyl-6-amino-4-(4-iodophenyl)-2,4-dihydropyrano[2,3-c]pyrazole-5-carbonitrile (4m)

Light yellow solid in (0.37 g, 86%); M.p. 250–252 °C; 1H NMR (500 MHz, CD_3OD-d_4): δ 1.69 (s, 3H, CH_3), 4.52 (s, 1H, 4H), 6.55–6.71 (m, 3H, Ar-H), 7.14 (t, 1H, Ar-H, $J = 11.5$ Hz) ppm; ^{13}C NMR (75 MHz, CD_3OD-d_4): δ 9.7, 37.4, 82.2, 114.8, 115.5, 117.2, 120.8, 125.9, 131.3, 138.9, 146.0, 151.4, 158.2, 162.3 ppm; MS m/z : 377.99 (M^+). Anal. Calcd for $C_{14}H_{11}IN_4O$: C, 44.46; H, 2.93; N, 14.82; Found: C, 44.37; H, 2.90; N, 14.79; HRMS (ES^+) Calcd for $(M + H)^+$ 379.1678 found m/z 379.1650.

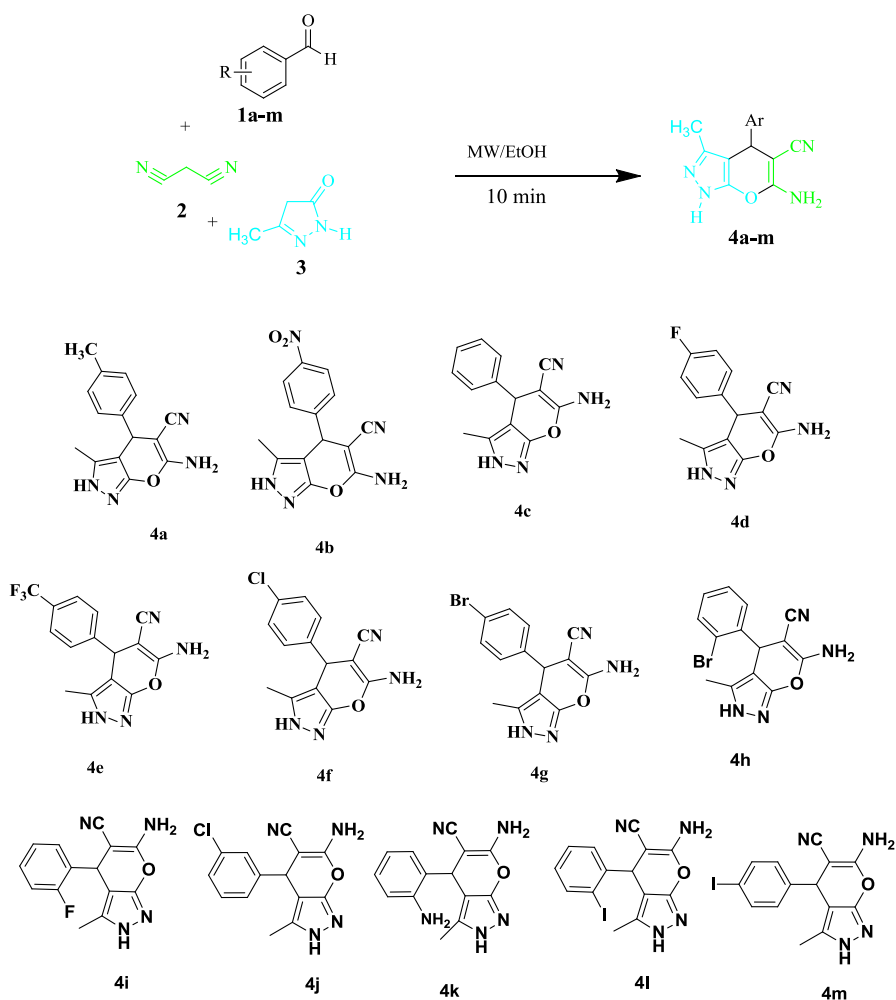
Biological experiment

By the agar well diffusion method [36, 37] against *Bacillus subtilis* (ATCC 6633), *Staphylococcus aureus* (ATCC 19433) (Gram-positive (G(+))), *Escherichia coli* (ATCC 8739), *Proteus vulgaris* (ATCC 29213) (Gram-negative (G(-))) bacterial stains, *Aspergillus niger* (MTCC 1881) and *Aspergillus flavus* (MTCC 1884) fungi were used to determine in vitro antibacterial and antifungal activities of reported compounds. In this, dimethyl sulfoxide was used as control and no visible inhibition zone was observed in control groups. Distilled water was used to prepare the test solutions. Two references, namely Chloramphenicol and Ciprofloxacin were used for antibacterial standard drugs and Ketoconazole and Fluconazole were used for antifungal standard drugs. A bacterial suspension was added to the sterile nutrient broth, and the mixture was poured into a Petri dish on a horizontal levelled surface. After the medium was solidified, wells of the dish were made in the agar medium. Subsequently, 25, 50, and 100 μ L of the reported compound's suspensions were loaded into the wells separately. The Petri dishes were incubated at 37 °C for one day for bacteria, and 28 °C for 48 h for fungi in an oven. After, appropriate incubation, the inhibition zone diameter of the well was measured. Experiments were carried out in triplicate and average zone diameters were measured.

Results and discussion

Synthetic results

All the targeted motifs **4(a–m)** were synthesized by a one-pot synthesis method using microwave irradiation to reduce the reaction time. Our successful efforts gave the products in quantitative yield within a short time of 10 min (Scheme 1). To a solution of methyl-1*H*-pyrazole-5(4*H*)-one (**3**) in ethanol were added arylaldehyde **1** and malononitrile (**2**), followed by irradiation to afford the pyranopyrazole derivatives **4(a–m)**. The proton NMR value at δ 4.71 ppm belongs to 4*H* hydrogen of the pyranopyrazole ring, and the peak appeared at δ 5.53 ppm due to the NH₂ group attached to the pyranopyrazole ring indicating the formation of product **4a**.



Scheme 1 Microwave synthesis of pyranopyrazole and their analogs

The other prepared compounds $4H$ proton range of δ 3.78–4.96 ppm and amino group protons range from δ 50.2 to 6.14 ppm revealed the formation of products **4(b–m)**. Total yields of the products were in the range of 92–81%. Moreover, bromo and chloro substituted compounds **4g** and **4j** were formed in the highest yields in comparison with those of other products. Thus, the present synthetic method may be used to prepare pyranopyrazole derivatives within a short time. All the compounds were characterized by proton NMR, carbon NMR, and mass elemental analysis.

Biological results

The compounds (Scheme 1) were screened for their in vitro antimicrobial activity against two Gram-positive, two Gram-negative bacteria, and two fungal strains. Most of the compounds showed excellent inhibitory antimicrobial activity against four bacterial and two fungal strains, few compounds displayed good antibacterial and antifungal activity, while some compounds were inactive against all strains. In this study, for comparison purpose, we were used two types of standard drugs for bacterial and for fungal uses. Biological results tabulated in Tables 1 and 2. From the data in Table 1, compound **4b** displayed higher antibacterial activity than other

Table 1 In vitro antibacterial activity of compounds **4(a–m)**

Compound no.	MIC in $\mu\text{g/mL}$ (Zone of inhibition in mm)			
	G (+)		G (–)	
	<i>B. subtilis</i> (ATCC-6633)	<i>S. aureus</i> (ATCC-19433)	<i>E. coli</i> (ATCC-8739)	<i>P. vulgaris</i> (ATCC-29213)
4a	–	–	–	–
4b	50 (15)	100 (16)	100 (15)	100 (15)
4c	–	–	–	100 (3)
4d	50 (7)	100 (5)	50 (6)	50 (8)
4e	100 (13)	25 (15)	100 (10)	100 (14)
4f	50 (10)	25 (11)	50 (10)	50 (12)
4g	50 (7)	100 (6)	100 (8)	100 (10)
4h	100 (7)	100 (7)	100 (6)	50 (8)
4i	100 (4)	50 (3)	25 (4)	100 (5)
4j	–	–	50 (3)	100 (3)
4k	–	–	–	–
4l	100 (8)	100 (8)	100 (9)	50 (10)
4m	50 (10)	100 (9)	100 (8)	100 (12)
Chloramphenicol	100 (22)	100 (18)	100 (19)	100 (14)
Ciprofloxacin	100 (21)	100 (20)	100 (17)	100 (13)
Control (DMSO)	–	–	–	–

MIC = minimum inhibitory concentration; G (+) = gram-positive; G (–) = gram-negative
 ‘–’ no activity

Table 2 In vitro antifungal activity of compounds **4(a–m)**

Compound no.	MIC in $\mu\text{g/mL}$ (zone of inhibition in mm)	
	Antifungal	
	<i>Aspergillus niger</i> (MTCC 1881)	<i>Aspergillus flavus</i> (MTCC 1884)
4a	–	50 (6)
4b	100 (26)	100 (30)
4c	–	–
4d	–	100 (10)
4e	100 (22)	50 (20)
4f	50 (16)	100 (17)
4g	100 (15)	100 (16)
4h	100 (9)	25 (9)
4i	25 (8)	100 (7)
4j	–	–
4k	–	–
4l	50 (11)	100 (9)
4m	100 (13)	100 (12)
Ketoconazole	100 (29)	100 (31)
Fluconazole	100 (28)	100 (34)
Control (DMSO)	–	–

active compounds. It exhibited higher antibacterial activity towards Gram-positive bacteria, against *Staphylococcus aureus* and its inhibition zone value of 16 mm at 100 $\mu\text{g/mL}$. In bacterial strains, an interesting point was noted that this compound displayed a greater inhibition zone than the standard drugs, namely, Chloramphenicol and Ciprofloxacin against *Proteus vulgaris* (ATCC 29213) Gram-negative bacteria strain and its zone of inhibition value of 15 mm at 100 $\mu\text{g/mL}$ concentration. The next lead antibacterial compound was **4e**, and it showed a second higher antibacterial inhibitory zone against all four bacterial strains. Besides, the best outcome of this motif was shown by an inhibition zone equal to Chloramphenicol bacterial standard, inhibition zone value 14 mm at 100 $\mu\text{g/mL}$ concentration and greater than Ciprofloxacin standard inhibition zone value 13 mm at 100 $\mu\text{g/mL}$. Meanwhile, compounds **4a**, and **4k** were inactive against all the bacterial strains. While the compound **4j** showed inhibition zone against Gram-negative bacteria, and the compound **4c** displayed antibacterial activity against *Proteus vulgaris* organism, in other organisms it was inactive. The compounds **4f**, **4l**, and **4m** were exposed for good antibacterial activity towards Gram-negative *Proteus vulgaris* organism with their inhibition zone values 12, 12 and 10 mm at a concentration of 50, 100, and 50 $\mu\text{g/mL}$. Attractively, the other compounds showed moderate to low antibacterial activities. In addition, compounds **4b**, and **4e** displayed higher antibacterial activity towards a gram-positive *Staphylococcus aureus* strain. But, the other active compounds showed a higher zone of inhibition

against *Proteus vulgaris* bacteria that did Gram-negative bacteria. Finally, the above results indicated that, compounds **4b**, and **4e** showed higher antibacterial activity than the other active compounds towards *Staphylococcus aureus* strain.

As presented in Table 2, the reported compounds screened for their antifungal minimal inhibitory concentrations (MIC $\mu\text{g/mL}$) and zone of inhibition (mm) against *Aspergillus niger* (MTCC 1881) and *Aspergillus flavus* (MTCC 1884) fungi's. The results revealed that some active compounds displayed higher antifungal activity towards *Aspergillus niger*, while, few other active compounds showed a higher inhibition zone against *Aspergillus flavus*. Among the tested compounds, compound **4b** showed a higher inhibition zone than the other active compounds. Its value was 30 mm at 100 $\mu\text{g/mL}$ towards *Aspergillus flavus* strain and in *Aspergillus niger*, its inhibition zone value was 26 mm at the same concentration. In addition, compound **4e** exhibited next the most inhibition zones than did the other active compounds of its value 22 mm towards *Aspergillus niger* at 100 $\mu\text{g/mL}$, and 20 mm against *Aspergillus flavus*. In this, the compound **4b** has the most active use against *Aspergillus flavus*, while, compound **4e** was a higher inhibition zone towards *Aspergillus niger* at the same concentration of 100 $\mu\text{g/mL}$. On the other hand, compounds **4f**, and **4g** displayed excellent antifungal activity and their inhibition zone values of 16, 17 mm at 50, 100 $\mu\text{g/mL}$ against *Aspergillus niger* fungi, and 15, 16 mm at 100 $\mu\text{g/mL}$ towards *Aspergillus flavus* strain. Besides compounds **4c**, **4j**, and **4k** were inactive against two fungal strains. Interestingly, compounds **4a**, and **4d** displayed an inhibition zone towards *Aspergillus flavus* only and those were inactive against another strain. Also, activity values of compounds **4a**, and **4d** were 6 and 10 mm at a minimal inhibitory concentration of 50 and 100 $\mu\text{g/mL}$. Compound **4m** exhibited an identifiable antifungal inhibition zone at 100 $\mu\text{g/mL}$ against all fungi for its values 13, and 12 mm. In addition, the other compounds displayed moderate antifungal activity against both strains.

Simulation results

In simulation studies, the electronic structural orientation, HOMO and LUMO orbital location of synthesized compounds were observed, along with these, were calculated their energies, HOMO–LUMO energy gap (E_g), dipole moment, and heat of formation (HF).

The most important parameters like electron densities and energies of frontier molecular orbitals are used for unsaturated structure to determine the reactive sites [38]. HOMO energy, and LUMO energy are related to ionization potential and electron affinity. While, the former energy is exemplifying the vulnerability of the molecule towards an attack by electrophiles whereas, the second one is towards attack by nucleophiles. According to the HOMO and LUMO data presented in Table 3, HOMO energy of compounds **4(a–m)** were ranged from -8.73 to -9.35 eV. In this, the high negative HOMO value -9.35 eV belonged to compound **4b**. Moreover, the compound **4e** has -9.24 eV HOMO energy, and the compound **4f** has -9.10 eV. The average ~ -9.06 eV of HOMO value corresponded to compounds **4d**, **4g**, **4h**, **4i**, and **4j**. Meanwhile, rest of the compounds have low negative HOMO energy. Further, compound **4b** showed the

Table 3 Simulation results of compounds **4(a–m)**

Compound	HF (kcal/mol)	HOMO (eV)	LUMO (eV)	E_g (eV)	Dipole moment
4a	62.738	– 8.906	0.003	8.909	4.251
4b	66.626	– 9.358	– 1.183	8.175	7.563
4c	72.480	– 8.957	– 0.040	8.917	4.371
4d	24.860	– 9.090	– 0.184	8.906	4.931
4e	– 88.826	– 9.246	– 0.610	8.636	6.146
4f	62.463	– 9.107	– 0.247	8.860	5.195
4g	75.520	– 9.098	– 0.247	8.851	5.111
4h	75.938	– 9.039	– 0.201	8.838	4.779
4i	26.039	– 9.044	– 0.144	8.900	4.584
4j	62.262	– 9.082	– 0.220	8.862	4.227
4k	62.842	– 8.916	– 0.014	8.902	4.130
4l	89.398	– 8.791	– 0.206	8.585	5.023
4m	88.154	– 8.753	– 0.255	8.498	5.309

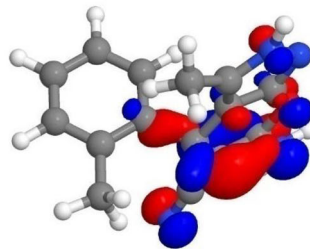
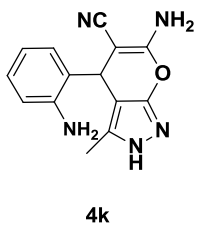
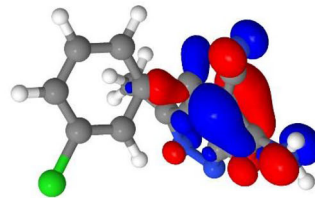
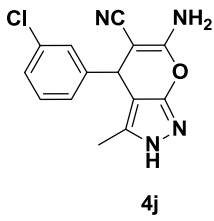
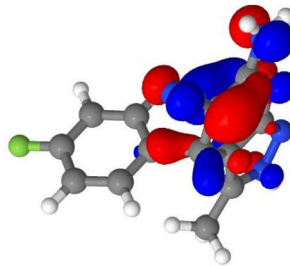
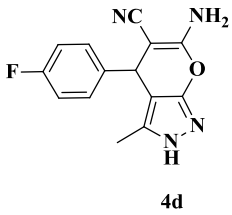
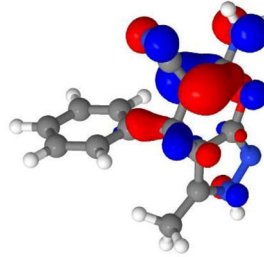
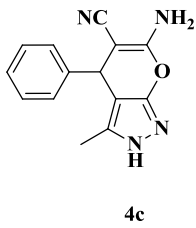
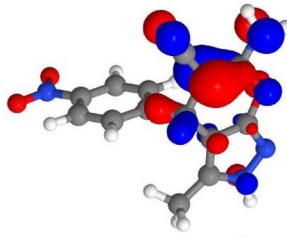
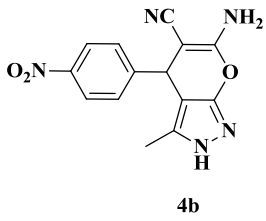
most negative LUMO energy value – 1.18 eV, and – 0.61 eV was the next lead LUMO energy corresponded to the compound **4e**. In the case of **4f**, **4g**, **4h**, **4j**, **4l**, and **4m** compounds, their LUMO energy was in the order **4m** > **4f** > **4g** > **4j** > **4l** > **4h**. Interestingly, compound **4a** has 0.003 eV of LUMO energy. At the same time, other compounds illustrated least negative LUMO energy value.

Accurately, the other important parameter is an energy gap (E_g) of HOMO and LUMO energies [39]. The E_g of all the reported molecules ranges from 8.17 to 8.91 eV, and, if the blend has a high reactivity, that means compound has a low energy gap. Similarly, the compound having a high energy gap leads to stumpy reactive nature or in another sense; a high strength of compounds has a low E_g vice versa.

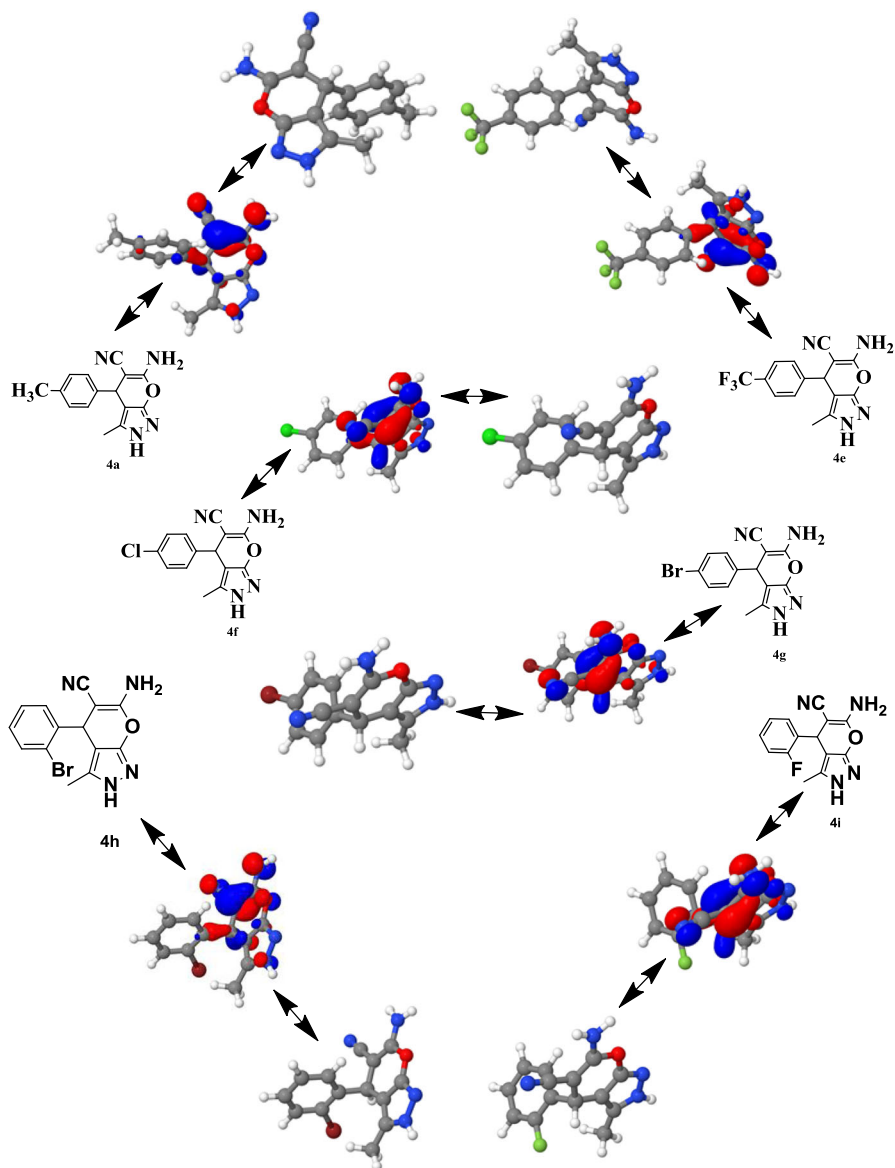
Furthermore, compounds dipole moment was calculated, and the dipole moment values range from **4.25** to **7.56** Debye. In addition, there was calculated HF of all the reported compounds (**4(a–m)**). Herein, compounds with varying activities have a very great dissimilarity in their HF. So, there was no clear relationship of HF and biological activity.

SARs discussion

To gain a better understanding of the antimicrobial capacity of pyranopyrazole derivatives, and search for potent derivatives, SARs is a key point. In all synthesized compounds **4(a–m)**, except **4l** and **4m**, the HOMO orbitals were situated on the fused ring (Structures **1** and **2**), whereas, the same orbitals of later compounds were located on an aryl group (Structures **3** and **4**). But, in case of LUMO orbitals, those were positioned differently with respect to the compounds, and; hence, there was no proper relation between the orbital orientation and biological results.



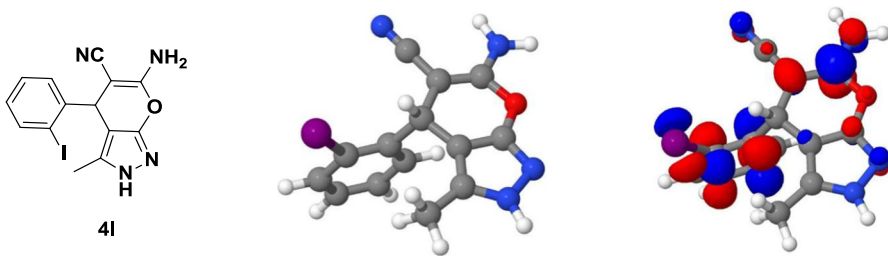
Structure 1 Electronic HOMO orbital location of compounds **4b**, **4c**, **4d**, **4j** and **4k**



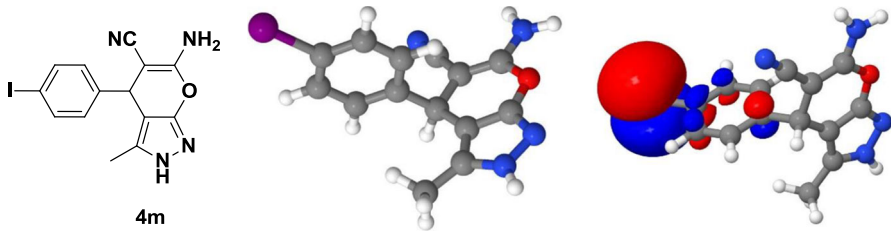
Structure 2 HOMO orbitals of compounds 4a, 4e, 4f, 4g, 4h and 4i

Dipole moment, lipophilic nature and their relationship with biological activity

For understanding the SARs of synthesized compounds and biological assay, dipole moment was the main parameter (Table 3) and this gave some acumen information about the compounds lipophilicity and hydrophilicity. Generally, lipophilic compounds are low dipole moment or a non-polar motif, while the hydrophilic



Structure 3 Electronic and HOMO orbital location of compound **4l**



Structure 4 Electronic and HOMO orbital location of compound **4m**

compounds are polar, and they will tend to have a polar bond with polar solvents like water, and; hence, makes it have a dipole moment. Moreover, hydrophilic compounds are of a water-soluble nature and if these compounds possess potent biological activity then, those are the most useful in the medicinal chemistry region for production of drugs. From the reported data, the lipophilic nature of the compound increases when the dipole moment decreases and leads to polarity decreases [40]. That means, as the high dipole moment leads to high polarity, for which in turn the lipophilic nature of the compound decreases, concludes the increases of hydrophilicity nature. Among the calculated compounds, compound **4b** has the highest dipole moment 7.56 Debye revealed that, the highest hydrophilic nature and dominant antimicrobial active compound. But, the compound **4k** was inactive, and it has a lipophilic nature that was due to its low dipole moment of 4.13 Debye. Besides, **4e** and **4m** compounds have apparent biological activity due to their excellent dipole moment of 6.14 and 5.30 Debye value and have the next higher hydrophilic nature. In fact, compounds **4f**, **4g** and **4l** showed dipole moment 5.19, 5.11 and 5.02 Debye, its hydrophilic order was **4f** > **4g** > **4l**, while the other compounds consisted of their dipole moments range of 4.93–4.22 Debye to show different antimicrobial activity.

HOMO–LUMO energy gap (vs) biological activity

The eventual charge transfer interaction in the molecule is responsible for bioactivity, which is explained by the decrease in HOMO and LUMO energy gap (E_g) [41, 42]. In reported compounds, compound **4b** has low E_g value 8.17 eV (Fig. 1) and was the highest potent antimicrobial agent. In fact, compounds **4e**, **4l**,

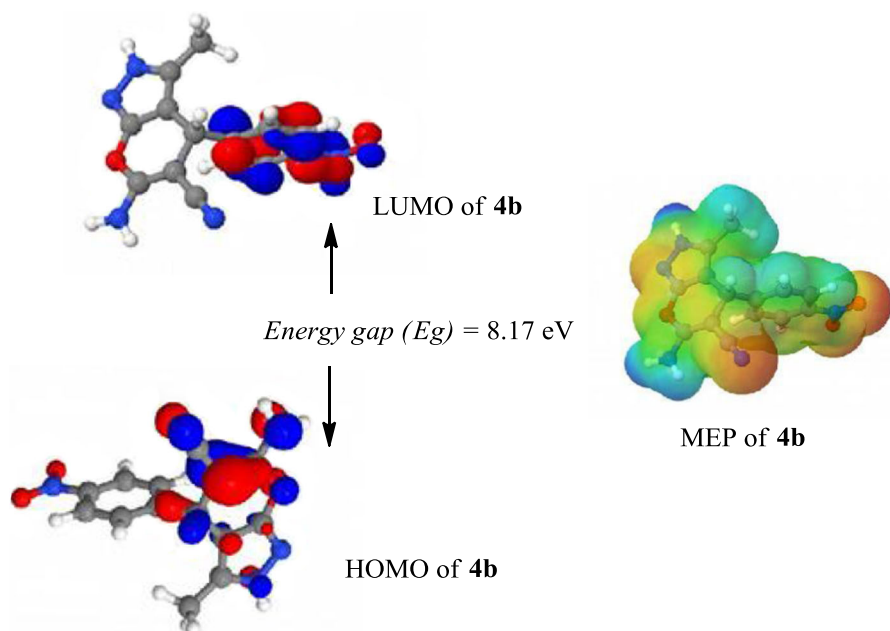


Fig. 1 Compound **4b**

and **4m** have the next lowest E_g values of 8.63, 8.58 and 8.49 eV and excellent antibacterial and antifungal activity. Further, the better E_g values showed compounds **4f**, **4g**, **4h** and **4j**, and their values of 8.86, 8.85, 8.83 and 8.86 eV, in decreased order of **4j** > **4f** > **4g** > **4h**. Not much difference in their E_g , exhibited different antimicrobial activity. On the other hand, compounds **4a**, **4c**, **4d**, **4i**, and **4k** have the E_g value range of 8.90–8.91 eV and exhibited moderate to low biological activity. Thus, compound **4b** has the low E_g value and higher antimicrobial activity and the compounds **4e**, **4l**, and **4m** displayed excellent biological activity due to their next low E_g values.

The justification of above results and their comparison with respect to each other explained that the correlation of simulation parameters with the biological data is a better way to classify the potent therapeutic compounds.

Conclusions

In this work, synthetic technique, simulation studies, antimicrobial activity and their connection to pyranopyrazoles were discussed. Screening of antimicrobial activity of targeted amalgams revealed that the compound **4b** produced higher antibacterial and antifungal activity than other active compounds. The electronic parameters supported this result. Dipole moment and the HOMO–LUMO energy gap revealed that **4b** has a dominant high dipole moment, hydrophilic nature and low energy gap (E_g). In addition, compound **4k** was inactive, and it has a lipophilic nature that was due to its low dipole moment. The rationale of these consequences clarified that

correlation of electronic results with biological data is a key technique to categorize the potent pharmaceutical drug compounds.

Acknowledgements Guda Mallikarjuna Reddy is grateful to the Brazilian Higher Education Personnel Training Coordination (CAPES: Coordenação de Aperfeiçoamento de Pessoal de Nível Superior) under the PNPd program and authors GMR and GS give thanks to Ural Federal University, Russia.

References

1. M.A. Fischbach, C.T. Walsh, *Science* **325**, 1089 (2009)
2. G.J. Armelagos, P.J. Brown, B. Turner, *Soc. Sci. Med.* **61**, 755 (2005)
3. A.H. Shamroukh, M.E.A. Zaki, E.M.H. Morsy, F.M. Abdel-Motti, F.M.E. Abdel-Megeid, *Arch. Pharm. Chem. Life Sci.* **340**, 345 (2007)
4. M.D. Aytemir, U. Calis, M. Ozalp, *Arch. Pharm. Chem. Life Sci.* **337**, 281 (2004)
5. F. Chabchoub, M. Messaad, H.B. Mansour, L. Chekir-Ghedira, M. Salem, *Eur. J. Med. Chem.* **42**, 715 (2007)
6. T.B. Prakash, G.D. Reddy, A. Padmaja, V. Padmavathi, *Eur. J. Med. Chem.* **82**, 347 (2014)
7. G.M. Reddy, P.R. Reddy, V. Padmavathi, A. Padmaja, *Arch. Pharm. Chem. Life Sci.* **346**, 154 (2013)
8. G.M. Reddy, A. Muralikrishna, V. Padmavathi, A. Padmaja, T.K. Tilak, C.A. Rao, *Chem. Pharm. Bull.* **61**, 1291 (2013)
9. G. Bertuzzi, E. Locatelli, D. Colecchia, P. Calandro, B.F. Bonini, J.Z. Chandanshive, A. Mazzanti, P. Zani, M. Chiariello, M. Comes, Franchini. *Eur. J. Med. Chem.* **117**, 1 (2016)
10. M.F. Khan, M.M. Alam, G. Verma, W. Akhtar, M. Akhter, M. Shaquiquzzaman, *Eur. J. Med. Chem.* **120**, 170 (2016)
11. G. Vasuki, K. Kumaravel, *Tetrahedron Lett.* **49**, 5636 (2008)
12. J.L. Wang, D. Liu, Z.J. Zhang, S. Shan, X.S.M. Srinivasula, C.M. Croce, E.S. Alnemri, Z. Huang, *Proc. Natl. Acad. Sci. U.S.A.* **97**, 7124 (2000)
13. E.S. El-Tamany, F.A. El-Shahed, B.H. Mohamed, *J. Serb. Chem. Soc.* **64**, 9 (1999)
14. Z.H. Ismail, G.M. Aly, M.S. El-Degwi, H.I. Heiba, M.M. Ghorab, *Egypt. J. Biotechnol.* **13**, 73 (2003)
15. M.E.A. Zaki, H.A. Soliman, O.A. Hiekal, A.E. Rashad, *Sect. C J. Biosci.* **61**, 1 (2006)
16. S.C. Kuo, L.J. Huang, H. Nakamura, *J. Med. Chem.* **27**, 539 (1984)
17. L. Bonsignore, G. Loy, D. Secci, A. Calignano, *Eur. J. Med. Chem.* **28**, 51 (1993)
18. H. Wamhoff, E. Kroth, C. Strauch, *Synthesis* **11**, 1129 (1993)
19. S.R. Mandha, S. Siliveri, M. Alla, V.R. Bommena, M.R. Bommineni, S. Balasubramanian, *Bioorg. Med. Chem. Lett.* **22**, 5272 (2012)
20. M. Mamaghani, R.H. Nia, F. Shirini, K. Tabatabaieian, M. Rassa, *Med. Chem. Res.* **24**, 1916 (2015)
21. X.H. Yang, P.H. Zhang, Z.M. Wang, F. Jing, Y.H. Zhou, L.H. Hu, *Ind. Crops Prod.* **52**, 413 (2014)
22. M.H. Helal, S.A. El-Awdan, M.A. Salem, T.A. Abd-elaziz, Y.A. Moahamed, A.A. El-Sherif, G.A.M. Mohamed, *SpectrochimicaActa Part A: Mol Biomol Spectrosc* **135**, 764 (2015)
23. Z. Yan, A. Liu, M. Huang, M. Liu, H. Pei, L. Huang, H. Yi, W. Liu, A. Hu, *Eur. J. Med. Chem.* **149**, 170 (2018)
24. P. Politzer, J.S. Murray, Z. Peralta-Inga, *Int. J. Quantum Chem.* **85**, 676 (2001)
25. P. Politzer, J.S. Murray, M.C. Concha, *Int. J. Quantum Chem.* **88**, 19 (2002)
26. S.P. Gejji, C.H. Suresh, K. Babu, S.R. Gadre, *J. Phys. Chem.* **103**, 7474 (1999)
27. J. Tomasi, R. Bonaccorsi, R. Cammi, in *Theoretical Models of Chemical Bonding*, ed. by R. Maksic (Springer, Berlin, 1990)
28. X.H. Liu, Y.M. Fang, F. Xie, R.R. Zhang, Z.H. Shen, C.X. Tan, J.Q. Weng, T.M. Xu, H.Y. Huang, *Pest Manag. Sci.* **73**, 1900 (2017)
29. X.H. Liu, Q. Wang, Z.H. Sun, D.E. Wedge, J.J. Becnel, A.S. Estep, C.X. Tan, J.Q. Weng, *Pest Manag. Sci.* **73**, 953 (2017)
30. X.M. Ding, Z.W. Zhai, L.P. Lv, Z.H. Sun, X.H. Liu, *Front. Chem. Sci. Eng.* **11**, 379 (2017)
31. A.K. Bhattacharjee, J.M. Karle, *Bioorg. Med. Chem.* **6**, 1927 (1998)
32. A.K. Bhattacharjee, J.M. Karle, *Chem. Res. Toxicol.* **12**, 422 (1999)
33. C.H. Suresh, A.M. Vargheese, K.P. Vijayalakshmi, N. Mohan, N. Koga, *J. Comput. Chem.* **29**, 1840 (2008)

34. M.S. Gordon, M.W. Schmidt, Chapter 41—advances in electronic structure theory: GAMESS a decade later, in *Theory and Applications of Computational Chemistry*, ed. by C.E. Dykstra, G. Frenking, K. S. Kim, G.E. Scuseria (Elsevier, Amsterdam, 2005), pp. 1167–1189
35. T. Noro, M. Sekiya, T. Koga, *Theor Chem Acc* **131**, 1 (2013)
36. K.T. Chung, W.R. Thomasson, C.D. Wu-Yuan, *J. Appl. Bacteriol.* **69**, 498 (1990)
37. C. Azoro, *World J. Bioechnol.* **3**, 347 (2002)
38. K. Fukui, T. Yonezawa, H.J. Shingu, *J. Chem. Phys.* **20**, 722 (1952)
39. Wahida Boufas, N. Dupont, M. Berredjem, K. Berrezag, I. Bechecker, H. Berredjem, N.E. Aouf. *J. Mol. Struct.* **1074**, 180 (2014)
40. M. Carcelli, P. Mazza, C. Pelizzi, G. Pelizzi, F. Zani, *J. Inorg. Biochem.* **57**, 43 (1995)
41. L. Padmaja, C. Ravikumar, D. Sajan, I.H. Joe, V.S. Jayakumar, G.R. Pettit, O.F. Nielsen, J. Raman *Spectrosc.* **40**, 419 (2009)
42. C. Ravikumar, I.H. Joe, V.S. Jayakumar, *Chem. Phys. Lett.* **460**, 552 (2008)

Affiliations

Guda Mallikarjuna Reddy^{1,2} · Gundala Sravya² · Gutha Yuvaraja³ · Alexandre Camilo Jr.⁴ · Grigory V. Zyryanov^{2,5} · Jarem Raul Garcia¹

- ¹ Department of Chemistry, State University of Ponta Grossa, Ponta Grossa, Parana 84030-900, Brazil
- ² Ural Federal University, Chemical Engineering Institute, Yekaterinburg, Russian Federation 620002
- ³ School of Chemical Engineering and Technology, Tianjin University, Tianjin 300072, People's Republic of China
- ⁴ Department of Physics, State University of Ponta Grossa, Ponta Grossa, Parana 84030-900, Brazil
- ⁵ I. Ya. Postovskiy Institute of Organic Synthesis, Ural Division of the Russian Academy of Sciences, 22 S. Kovalevskoy Street, Yekaterinburg, Russian Federation 620219